The research of Fuzzy Immune Linear Active Disturbance Rejection Control Strategy for three-motor synchronous system

Li Hui*, Liu Xingqiao*, Li Jing**

** School of Electrical and Information Engineering, Jiangsu University ,Zhenjiang 212013, China (Tel: 13645234923; e-mail: 13645234923@ 163.com).*
*** Faculty of Electronic and Electrical Engineering, Huaiyin Institute Of Technology ,HuaiAn 223003, China (e-mail: lijing_1981_312@163. com)*

Abstract: For the shortage of traditional Proportion Integration Differentiation (PID) in the application of the current multi-motor synchronous control system, this paper proposes a new control method which is fuzzy immune linear active disturbance rejection control (FI-LADRC) technology. The modern fuzzy immune control theory and active disturbance rejection control technology is combined for achieving the precise control of the three-motor synchronous coordination system. According to three motor synchronous system mathematical model, the whole disturbances compensation and the strong decoupling of the master motor speed and tension are achieved by the use of extended state observer (ESO). Moreover, nonlinear intelligent feedback is achieved by taking modern fuzzy immune control technology. Simulations and experiments show that: the control performance of the system is significantly better than the one of traditional PID control, such as good dynamic performance, obvious decoupling effect, strong anti-interference ability, high tracking accuracy, fast response and good robustness.

Keywords: fuzzy immune, ADRC, accuracy control, decoupling effect.

1. INTRODUCTION

With the rapid development of industrial automation, in many industrial automation occasions, such as paper mill, iron and steel industry and other industry occasions dealing with stretching and rolling, that only one motor is controlled has been unable to meet the modern industrial production requirements. The application of multi-motor synchronous control is becoming more and more extensive. The control performance of the system will directly affect the quality of the product. Therefore, multi-motor synchronous control strategy is of great importance.

Multi-motor synchronous system is a multi input-multi output, time-varying, nonlinear and complex system. How to solve the decoupling of the main parameters and improve the tracking accuracy, anti-interference ability are the main problems of the multi-motor synchronous control. Currently there are many control strategies for it. Traditional PID control method is a simple control method and suitable for linear time-invariant control system. But PID can not online adjust the parameters of the control system for the change of on-site control environment, so robust performance of PID is poor.With the development of modern control theories, more and more advanced control methods are introduced, e.g., artificial immune control (CHEN Shao-bai et al., 2006), fuzzy immune PID control (Xia Changliang et al., 2007; LI Hong-bin et al., 2008), ADRC control (J. Han, 2009; Dan Wu et al., 2009; LIU Xing-qiao et al., 2010,2012; Shihua Li et al., 2012; Marco Pizzocaro et al., 2013). ADRC was initially proposed by HAN (J.HAN, 1999) and Gao et al., (Z. Gao, 2001) using nonlinear gains and was simplified by Gao (Z. Gao, 2003, 2006). ADRC is the improvement of the traditional PID control. ADRC was used for decoupling in hot rolling mill (WANG Li-jun, 2012). For the three-motor synchronous control, the first-order optimized ADRC technology was developed (LIU Xing-qiao et al., 2010), and second-order ADRC control scheme was proposed (LIU Xing-qiao et al., 2010), and fuzzy ADRC was presented (Xingqiao Liu et al., 2011) .

On the basis of previous work, a new control scheme(FI-LADRC) is proposed which combines fuzzy immune control technology with linear ADRC. There are many advantages, e.g., strong decoupling ability, strong anti-interference capability, and high tracking accuracy. Simulation and experiment comparisons are presented to verify that FI-LADRC control scheme is an effective control method in the field of multi-motor synchronous coordinate control.

This paper is organized as follows: In the first section, this issue and the previous work done are introduced in detail. And in the Section 2, the mathematical model is introduced. The design of FI-LADRC control scheme is presented in Section 3. The tuning of control parameters about FI-ADRC and traditional PID are finished in Section 4. System stability is proved in Section 5. Simulation and experiment results and Analysis are provided in Section 6 and Section 7. Conclusion are given in Section 8.

2. THREE-MOTOR SYNCHRONOUS CONTROL SYSTEM MATHEMATICAL MODEL

System hardware model is shown in Fig.1. Three Micro-master Vector (MMV) inverters respectively drive three motors. Motor 1 is the master motor, motor 2 and motor 3 are slave motors. Thus, motor 1 is called main motor.

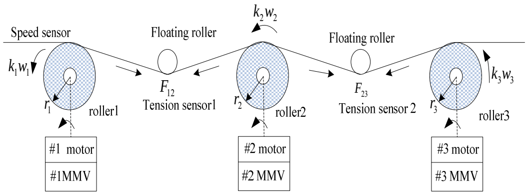

Fig. 1. The model of three motor synchronous system.

Three motors jointly drive one conveyer belt after they are decelerated in 15:1 ratios by reduction boxes, and floating rollers strain the conveyer belt to increase the friction between the conveyer belt and the driving rollers (Liu Xing-qiao et al.,2011). Three-motor synchronous system model in the d, q synchronous rotating coordinate system can be expressed in (1).

$$\begin{cases}\dot{\omega}_{r1}=\dfrac{n_{p1}}{J_1}\left[\left(\omega_1-\omega_{r1}\right)\dfrac{n_{p1}T_{r1}}{L_{r1}}\Psi_{r1}^2-\left(T_{L1}+r_1F_{12}\right)\right]\\ \dot{\omega}_{r2}=\dfrac{n_{p2}}{J_2}\left[\left(\omega_2-\omega_{r2}\right)\dfrac{n_{p2}T_{r2}}{L_{r2}}\Psi_{r2}^2-\left(T_{L2}+r_2F_{23}-r_2F_{12}\right)\right]\\ \dot{\omega}_{r3}=\dfrac{n_{p3}}{J_3}\left[\left(\omega_3-\omega_{r3}\right)\dfrac{n_{p3}T_{r3}}{L_{r3}}\Psi_{r3}^2-\left(T_{L3}-r_3F_{23}\right)\right]\\ \dot{F}_{12}=\dfrac{K_1}{T_1}\left(\dfrac{1}{n_{p1}}r_1k_1\omega_{r1}-\dfrac{1}{n_{p2}}r_2k_2\omega_{r2}\right)-\dfrac{F_{12}}{T_1}\\ \dot{F}_{23}=\dfrac{K_2}{T_2}\left(\dfrac{1}{n_{p2}}r_2k_2\omega_{r2}-\dfrac{1}{n_{p3}}r_3k_3\omega_{r3}\right)-\dfrac{F_{23}}{T_2}\end{cases} \quad (1)$$

Here F_{12} is the tension between motor 1 and motor 2; F_{23} is the tension between motor 2 and motor 3; Suppose three motors numbered i ($i=1,2,3$), ω_{i} are respectively synchronous rotational angular velocity of the three motors; ω_{ri} are respectively the rotor electrical angular velocity of the three motors ; Ψ_{ri} and J_{i} are respectively the rotor flux and the moment of inertia of the three motors; T_{Li} and T_{ri} are respectively the load torque and the motor time constant of the three motors; L_{ri} and n_{pi} are respectively rotor inductance and the number of pole-pairs of the three motors; k_{i} denote speed ratio between three motors; r_{i} respectively denote roller radius of the three motors.

T_1 and T_2 denote change rates of the tension;

K_1 and K_2 denote transfer coefficients;

3. FI-LADRC CONTROL SCHEME

The overall structure and design method of FI-LADRC is described in this chapter.

3.1 Overall structure of the control system

Control system is composed of fuzzy immune ADRC control model and three motor synchronous system. The structure is shown in Fig.2.

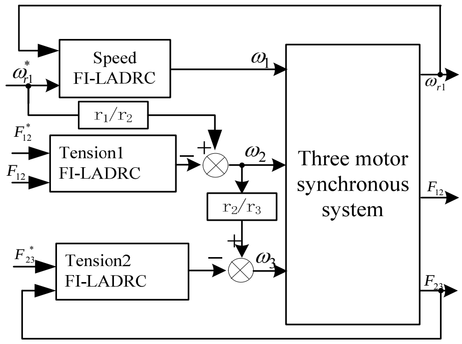

Fig. 2. The frame of the whole control system.

3.2 First order FI-LADRC

ADRC is composed mainly of tracking differentiator (TD), extended state observer (ESO), non-linear error feedback (NLSEF), and disturbance compensation (Jingqing Han, 2008). In this paper, the first-order linear ARDC is used. Second-order linear ESO(LESO) is used according to first-order ADRC. There is no derivative output in LESO unit. And the main role of TD unit lies in arranging transition process. But for the multi-motor synchronous control system, arranging the transition process is not necessary. Therefore, TD unit can be omitted, and the same time NLSEF unit can be replaced by the fuzzy immune nonlinear proportion control unit.

Specific structure is shown in Fig.3. It combines the advantages of LADRC control theory and modern fuzzy immune control theory. The control system has strong anti-interference ability and decoupling control ability. Moreover, the control algorithm is simple because of using LADRC.

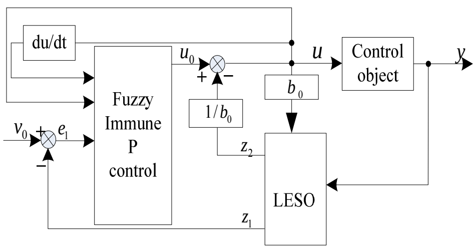

Fig. 3. The frame of the FI-LADRC.

According to (1), the control object can be written as

$$\begin{aligned}x^{(n)} &= g_0(x^{(0)},x^{(1)},\ldots,x^{(n-1)},t)+b_0u\\ &+g_1(x^{(0)},x^{(1)},\ldots,x^{(n-1)},w(t))+b_1u\end{aligned} \quad (2)$$

Where $g_0(x^{(0)},x^{(1)},...,x^{(n-1)},t)+b_0u$ denotes the part of known, and $g_1(x^{(0)},x^{(1)},...,x^{(n-1)},w(t))+b_1u$ denotes the part of the unknown. u denotes the input signal. $w(t)$ is the unknown disturbance. The unknown disturbance signal can be expanded to the new state by designing LESO.

3.2.1 Design of LESO

In LADRC control, LESO plays an important role, and expands the whole output disturbances to a new state z_2. And then observation value is compensated in the system. It is not necessary to know the specific mathematic model of the disturbance, and it is not need to measure disturbance directly. The disturbances are estimated according to the controller input and the system output feedback. And dual-channel compensation is applied in LADRC. Specific design algorithm is shown in (3).

$$\begin{cases} e_1 = z_1 - y \\ z_1 = z_1 + h \times (z_2 - \beta_{01} \times e_1 + b_0 \times u) \\ z_2 = z_2 - h \times \beta_{02} \times e_1 \end{cases} \tag{3}$$

Where e_1 denotes the observation error, z_1 denotes the tracking signal of the output signal y, z_2 denotes the observed value for the sum of the disturbances, h denotes sample time of the system. b_0 denotes the compensation factor. β_{01} and β_{02} denote the output error correction gain.

3.2.2 Nonlinear Fuzzy immune control

Modern immune control is nonlinear proportion control based on the principle of biological immune. It makes actual target as an antigen. The antibodies are the key of the problem. Biological immune system can produce antibodies to resist the foreign invasion antigens. Organism's immune system is composed of the lymphocytes and antibody molecules. Lymphocytes are composed mainly of T cells and B cells, and T cells are divided into T_H (assistant cells) and T_S (inhibition cells). B cells are stimulated to active and breed when antigens enter the body and are digested by the surrounding cells. And then B cells produce antibodies to eliminate antigens. When the antigens are more, T_H cells becomes more, T_S cells become fewer. Therefore, more B cells are produced. On the contrary, T_H cells become fewer. T_S cells become more. And fewer B cells are produced for reaching equilibrium after a period of time (LI Hong-bin et al., 2008).

Immune control achieves a good control effect by the use of adaptive adjustment parameter function which can resist antigens in immune system. Thus, the control system has strong robustness.

The $e(k)$ is made as antigens. Total stimulus $S(k)$ came from B cells is made as control input $u(k)$. $T_H(k)$ is the output signal of the T_H cells stimulated by antigens. And there is (4).

$$T_H(k) = k_1 e(k) \tag{4}$$

Where k_1 is positive promotion coefficient.

The impact of the T_S cells on the B cells is $T_S(k)$. And there is (5).

$$T_S(k) = k_2 f(u(k), \Delta u(k)) e(k) \tag{5}$$

Where k_2 is a positive suppression coefficient, f is a non-linear function.

The whole stimulus received by B cells can be written as (6).

$$S(k) = T_H(k) - T_S(k) = u(k) \tag{6}$$

Thus, there is (7).

$$\begin{aligned} u(k) &= k_1 - k_2 f(u(k), \Delta u(k)) \\ &= K(1 - \eta f(u(k), \Delta u(k))) \end{aligned} \tag{7}$$

Where $K = k_1$, K can be expressed as the response speed. $\eta = k_2 / k_1$, η determines the stabilization degree of the system.

From the above equations it can be known that immune control is essentially nonlinear proportion control. Now the main problem to be solved is how to express the nonlinear function f. The system uses fuzzy controller to approximate f. Each of input variables is expressed two logic value, namely "positive" (P) and "negative" (N). The output variables can be expressed three logic value, namely "positive" (P), "zero" (Z) and "negative" (N). Membership function is shown as Fig.4 and Fig.5.

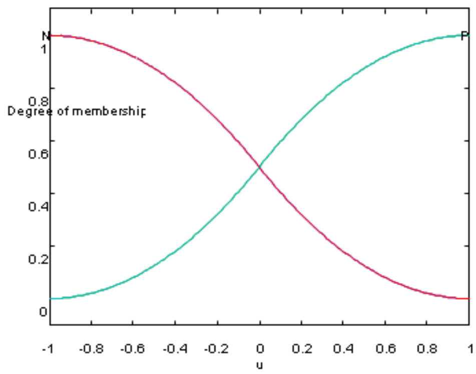

Fig. 4. The membership function of input variable.

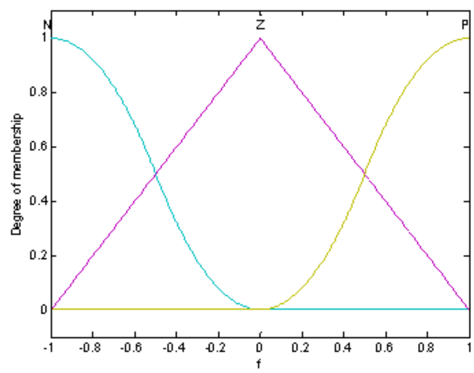

Fig. 5. The membership function of output variable.

The fuzzy rules can be expressed as Table 1.

Table 1. Fuzzy Rules.

u	Δu	*f*
P	P	N
P	N	Z
N	P	Z
N	N	P

3.2.3 The design of the total controller output

Combining the equations of ADRC with the equations of fuzzy immune control, the whole control equations of the system can be achieved as (8).

$$\begin{cases} e_1 = z_1 - y \\ z_1 = z_1 + h \times (z_2 - \beta_{01} \times e_1 + b_0 \times u) \\ z_2 = z_2 - h \times \beta_{02} \times e_1 \\ u = K \times (1 - \eta \times f(u, \Delta u)) - z_2 / b_0 \end{cases} \tag{8}$$

4. TUNING OF CONTROL PARAMETERS

4.1 FI-ADRC Control Parameters Tuning

Control parameters in the control system include fuzzy immune control parameters (K_i, η_i)($i = 1,2,3$), as well as the ESO parameters(β_{i1} , β_{i2}). According to (Jingqing Han, 2008), simulation study of ESO shows that β_{i1} is inversely proportional to the sampling step h , and β_{i2} is inversely proportional to $1/5h^2$. Here, we take $h = 0.1$s . Thus, β_{i1} is selected as 10, and β_{i2} is selected as 20. The parameter K_i of the fuzzy immune control directly affects the speed of response of the control system, and indirectly affects the steady-state error. η_i affects the stabilization degree of the system. Tuning appropriately the value of η_i to larger can suppress overshoot of the system. To a certain extent, it is an advantage of fuzzy immune ADRC scheme which can be used to solve the conflict between the response speed and the overshoot by adjusting the parameters(K_i, η_i).

In line with this principle, the parameters are selected as:

Main motor speed controller parameters:

$$K_1 = 1.8, \eta_1 = 0.6, \beta_{01} = 10, \beta_{02} = 20 \tag{9}$$

Tension controller 1 parameters:

$$K_2 = 8.0, \eta_2 = 0.6, \beta_{11} = 10, \beta_{12} = 20 \tag{10}$$

Tension controller 2 parameters:

$$K_3 = 5.0, \eta_3 = 0.8, \beta_{31} = 10, \beta_{32} = 20 \tag{11}$$

4.2 Traditional PID Control Parameters Tuning

For traditional PID control parameter tuning, engineering tuning method is used in three control modules(main motor speed control module, tension controller 1 module and tension controller 2 module) respectively. And the control parameters which have been tuned are shown as follows:

Main motor speed controller parameters:

$K_{p1} = 6.7, K_{i1} = 0.1, K_{d1} = 0.04$

Tension controller 1 parameters:

$K_{p2} = 8.0, K_{i2} = 0.4, K_{d2} = 11.4$

Tension controller 2 parameters:

$K_{p3} = 5.0, K_{i3} = 0.4, K_{d3} = 12.7$

5. PROOF SYSTEM STABILITY

The design of stability is very necessary for the control system. The following equations can be deduced from (8).

Firstly, control signal may be expressed as (12).

$$\omega_i = K_i(1 - \eta_i f_i)(\omega_i - z_{1i}) - \dot{z}_{2i} / b_i \tag{12}$$

Where z_{1i} is the tracking signal of ω_{ri} . b_i is the compensation factor of ADRC. It is shown that follows ω_{ri} is followed by z_{1i} in (Jingqing Han, 2008). So it can be assumed that $z_{1i} = \omega_{ri}$. z_{2i} is the observation value of disturbances in LESO. After the affect of the known part is excluded, the observations of ESO can be taken as load disturbances. $z_{2i} = T_{Li}$. The load disturbances can be put into the control signal expression. Thus, there is (13).

$$\omega_i = K_i(1 - \eta_i f_i)(\omega_i - \omega_{ri}) - T_{Li} / b_i \tag{13}$$

Here f_i (i = 1,2,3) are the three non-linear functions of fuzzy immune control. And they are achieved by the fuzzy algorithm. There is (14).

$$-1.0 \le f_i \le 1.0, \ K_i > 0, \ \eta_i > 0 \tag{14}$$

The mathematical model of the system in section 2 can be rewritten as (15).

$$\begin{aligned} \dot{X} &= AX + BU + CI \\ Y &= DX \end{aligned} \tag{15}$$

Here, $X = (\omega_{r1} \ \omega_{r2} \ \omega_{r3} \ F_{12} \ F_{23})^T$, $U = (\omega_1 \ \omega_2 \ \omega_3)^T$. Put the simulation parameters into (15), and then the original system matrix (16) can be obtained.

$$A = \begin{bmatrix} -0.6224 & 0 & 0 & -0.09 & 0 \\ 0 & -0.6224 & 0 & 0.09 & -0.09 \\ 0 & 0 & -0.6224 & 0 & 0.09 \\ 0.03 & -0.03 & 0 & -1.0 & 0 \\ 0 & 0.03 & -0.03 & 0 & -1.0 \end{bmatrix} \tag{16}$$

In the matlab environment all eigenvalues of ***A*** can be obtained by using eig function, which is (-0.9927, -0.9772, -0.6452, -0.6224, -0.6297). And all of them are negative. From these it can be seen that system matrix ***A*** is negative definite matrices.

If (12) is put into the control system, and then the new system matrix B will be obtained as (17).

$$B = A - \begin{bmatrix} K_1(1-\eta_1 f_1) & 0 & 0 & 0 & 0 \\ 0 & K_2(1-\eta_2 f_2) & 0 & 0 & 0 \\ 0 & 0 & K_3(1-\eta_3 f_3) & 0 & 0 \\ 0 & 0 & 0 & 0 & 0 \\ 0 & 0 & 0 & 0 & 0 \end{bmatrix} \tag{17}$$

Obviously, $\begin{bmatrix} K_1(1-\eta_1 f_1) & 0 & 0 & 0 & 0 \\ 0 & K_2(1-\eta_2 f_2) & 0 & 0 & 0 \\ 0 & 0 & K_3(1-\eta_3 f_3) & 0 & 0 \\ 0 & 0 & 0 & 0 & 0 \\ 0 & 0 & 0 & 0 & 0 \end{bmatrix}$ is a Diagonal matrix. Thus, ***B*** is negative definite matrix as long as $K_i(1-\eta_i f_i) > 0$. And all eigenvalues lie in the left half plane as long as ***B*** is negative definite matrix. And finally the system is stable as long as $K_i(1-\eta_i f_i) > 0$.

There is $-1.0 \le f_i \le 1.0,\ K_i > 0,\ \eta_i > 0$.

Therefore, $K_i(1-\eta_i f_i) > 0$ can be deduced as long as $0 < \eta_i < 1$.

There is $\begin{matrix} \eta_1 = \eta_2 = 0.6 \\ \eta_3 = 0.8 \end{matrix}$ in section 4. The parameters of η_i are all lie in [0,1]. Thus the whole control system is stable.

6. SIMULATION AND ANALYSIS

In simulink environment the system model is made by S-function. And some simulations and analysis are made for decoupling characteristics, anti-jamming capability, and tracking ability.

Select the motor parameters as (18).

$$\begin{aligned} & L_{r1} = L_{r2} = L_{r3} = 0.58\,\mathrm{H} \\ & n_{p1} = n_{p2} = n_{p3} = 2 \\ & J_1 = J_2 = J_3 = 0.5\,\mathrm{kg \cdot m^2} \\ & T_1 = T_2 = 1 \\ & k_1 = k_2 = k_3 = 1/15 \\ & r_1 = r_2 = r_3 = 0.09\,\mathrm{m} \\ & T_{r1} = T_{r2} = T_{r3} = 0.05 \\ & \psi_{r1} = \psi_{r2} = \psi_{r3} = 0.95\,\mathrm{Wb} \end{aligned} \tag{18}$$

6.1 Decoupling Performance Simulation and Analysis

First, the reference tension F_{12} between the main motor and the second motor keeps 15 kg, and the reference tension F_{23} between the second motor and the third motor keeps in 10 kg. The main motor reference speed is increased suddenly from 300r/min to 400r/min at 40th second. Speed-tension response curves of traditional PID control and FI-LADRC control are presented in Fig.6(a) and (b).

As can be seen from the curves that tension of traditional PID control is affected much than the one of FI-LADRC when the main motor speed is increased suddenly. And the curves of FI-LADRC are more stable than the one of traditional PID. Thus, it can be seen that the decoupling capability of FI-LADRC is better than the one of traditional PID scheme. Meanwhile, from the curves it can be seen that to FI-LADRC scheme, the response is fast, and the overshoot is small, and the settling time is short. Thus, it is obviously that the dynamic performance of FI-LADRC is much better than the one of traditional PID scheme. The detail data is shown in Table 2. And the same time the FI-LADRC can solve effectively the contradiction between system response speed and overshoot.

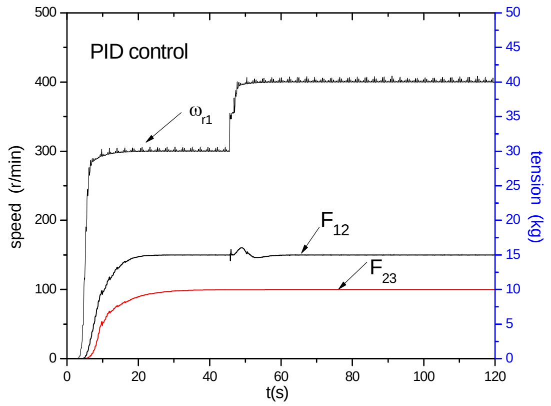

(a)PID control

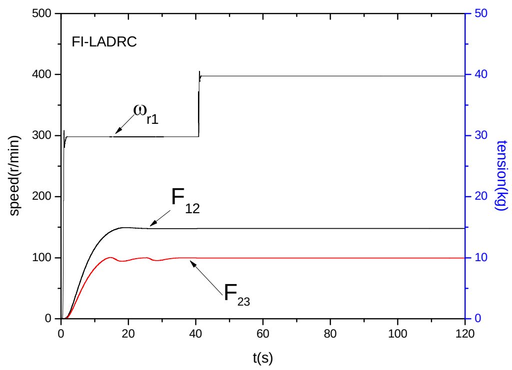

(b) FI-LADRC

Fig. 6. Speed-tension curves when the tension is fixed and the speed is increased suddenly.

Table 2. Dynamic performance comparison between FI-LADRC and PID control in simulation.

Control scheme	Rising time(s)	overshoot
FI-LADRC	0.8	1.41%
PID	9.77	2%

6.2 Anti-jamming ability Simulation and Analysis

Simulation time is 120 seconds. A test is made: a disturbance signal is added on the main motor speed at 70th second, which is a triangular signal with 300 amplitude and 1 second plus width. The response curves of FI-LADRC and traditional PID are shown in Fig.7(a) and (b).

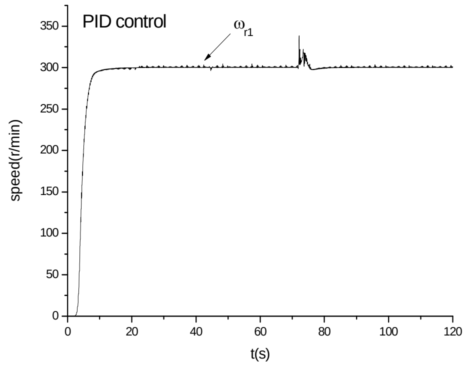

（a）PID control

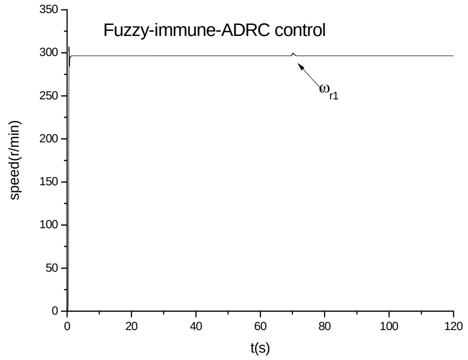

（b）FI-LADRC

Fig. 7. The response curves of the anti-jamming ability simulation.

As can be seen from Fig.7, the maximum disturbance response of tradition PID control reaches 7.3%; However, the maximum disturbance response of FI-LADRC only reaches 1%. From this it can be seen that the anti-jamming ability of FI-LADRC is stronger than the one of traditional PID scheme. And because of the adaptive regulation function of immune control, FI-LADRC control system has strong robustness.

6.3 Tracking Performance Simulation and Analysis

Simulation time is 25 seconds. The main motor reference speed adopts the triangular wave signal whose amplitude rises from 0 r/min to 500r/min and then descends from 500 r/min downto 0 r/min. The tracking tests of traditional PID control and FI-LADRC are made. And the response curves are shown in Fig.8 (a) and (b).

As can be seen from Fig.8 that the tracking accuracy of FI-LADRC is higher than the one of traditional PID control. The tracking performance is shown in Table 3.

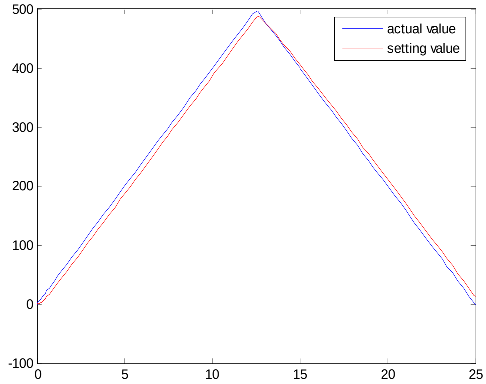

（a）PID control

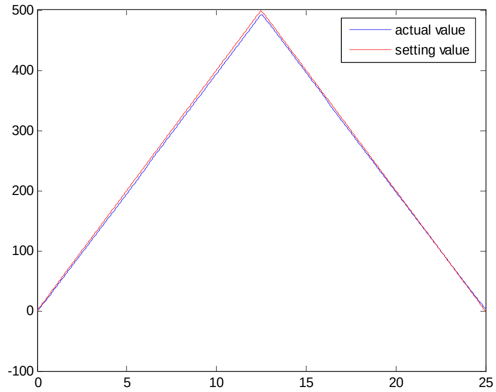

（b）FI-LADRC

Fig. 8. The curves of the tracking simulation.

Table 3. Tracking performance comparison in simulation.

Control scheme	Tracking error(r/min)
FI-LADRC	±4.45 r/min
PID	±11.2 r/min

7. EXPERIMENTS AND ANALYSIS

In order to further prove the performance of FI-LADRC, some experiments are done accordingly. The experimental platform is built with Siemens PLC-300, three inverters, and three AC induction motors. And the experimental platform is shown in Fig.9. The tensions between two motors are measured by tension sensor SL100. The speed of the main motor is measured by a circular grating incremental encoder. PLC-300 is connected to three inverters via Profibus. PLC-300 send commands to three inverters according to the control shemes for driving three AC induction running. Moreover, speed signal from a circular grating incremental encoder and tension signals from SL100 are conditioned and then transmitted to PLC-300.

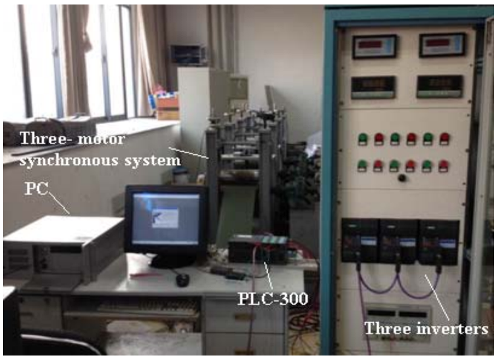

Fig. 9. Picture of experimental platform.

7.1 Decoulping experiment

Decoulping experiment is done while the main motor reference speed keeps 300 r/min and the reference tensions are changed suddenly. At 80th second, the reference tension F_{12} between the main motor and the second motor descends from 15 kg downto 13 kg, And the reference tension F_{23} between the second motor and the third motor descends from 12 kg downto 10 kg. The result is shown in Fig.10 (a) and (b).

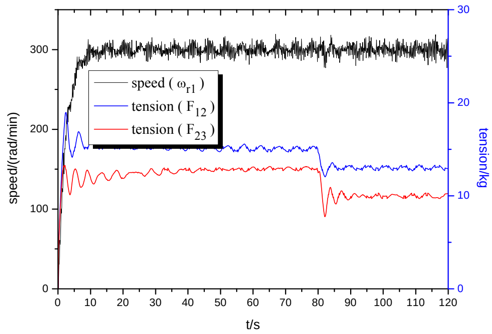

(a)PID control

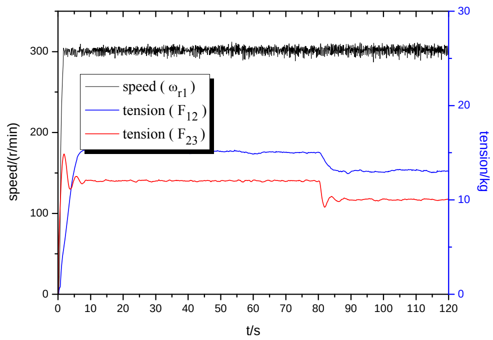

(b) FI-LADRC

Fig. 10. The experimental curves of speed-tensions.

From Fig.10 it can be seen that the speed using FI-LADRC is changed smaller than the one using traditional PID control when the tensions are all changed suddenly. Thus, it can be known that the decoulping effect of FI-LADRC is better than PID control. And the same time the respond speed of FI-LADRC is faster than the one of PID control.

7.2 Tracking experiment

Next, the tracking experiment is done for the main motor speed controller. The reference signal is composited by the step signal and the triangle signal. And before 40th second, the reference signal is a step signal whose amplitude is 400 r/min. After 40th second, the reference signal is a triangle signal whose amplitude is 200 r/min to 400 r/min and the period is 40 seconds. The scheme of FI-LADRC and tradition PID are used to make a experiment for tracking performance. The response curves are shown in Fig.11 (a) and (b).

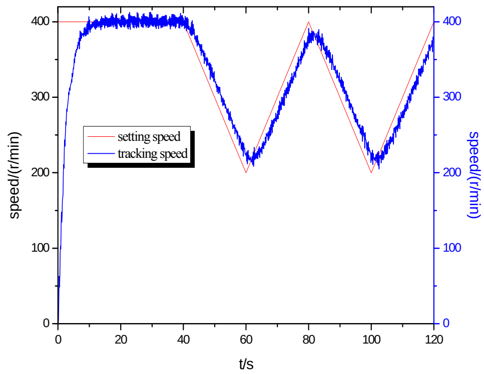

(a)PID control

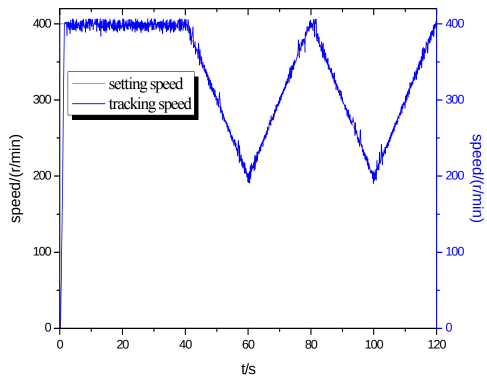

(b) FI-LADRC

Fig. 11. The experimental curves of tracking performance experiment.

As can be seen from Fig.11 (a) and (b) that the tracking performance of FI-LADRC is much better than the one of traditional PID control. And for FI-LADRC, the rising time is much shorter than the one of traditional PID control. In addition, the overshoot is much smaller than the one of traditional PID control. The detail data is shown in Table 4.

Table 4. Experimental tracking performance comparison

Control scheme	Tracking error	Rising time(second)	overshoot
FI-LADRC	±2.5%	1.6	1.72%
PID	±6.4%	9.5	3.34%

7.3 Anti-jamming ability experiment

Finally, Anti-jamming ability experiment is done for the main motor speed controller. The reference signal is a step signal whose amplitude is 300 r/min. Jam signal is a signal whose amplitude is 100 r/min at 40th second. The scheme of FI-LADRC and tradition PID are used to make a experiment for testing anti-jamming ability. The response curves are shown in Fig.12 (a) and (b).

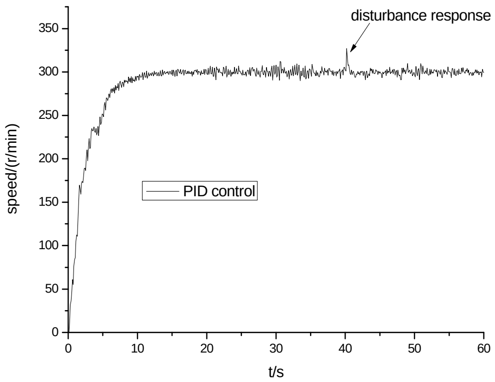

(a)PID control

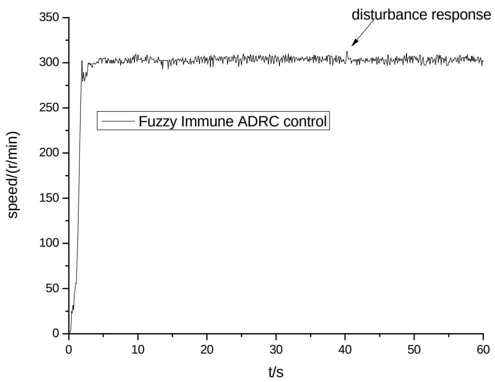

(b) FI-LADRC

Fig. 12. The experimental curves of anti-jamming ability experiment.

From Fig.12 (a) and (b) as can be seen that the response amplitude of FI-LADRC and traditional PID which is caused by jam signal are about 12.82 r/min and 26.95 r/min respectively. Therefore, it is obviously that the anti-jamming ability of FI-LADRC is much better than the one of traditional PID control.

8. CONCLUSION

This paper presents FI-LADRC strategy for three-motor synchronous system. Linear ADRC and fuzzy immune control theory are combined to solve the contradiction between the response speed and the system overshoot. Simulation and experiment results show that: FI-LADRC control strategy can successfully achieved decoupling of speed and tension. The control system using FI-LADRC has strong anti-jamming capability, good dynamic performance, and high tracking precision. Thus, it is obviously that FI-LADRC is a new viable method for multi-motor synchronous control.

ACKNOWLEDGEMENT

This research was financially supported by National Natural Science Foundation of China(60874014、51273154), Huaian agricultural science and technology guidance project(HANZ2014007), Jiangsu Province 2013 Graduate Students Research and Innovation Program(CXLX13_669), Jiangsu Agricultural Science and Technology Support Project（BE2013402）.

REFERENCES

Chen Shao-bai，Tan Guang-xing，Mao Zong-yuan. (2006). Optimizing Parameters of PID Controller Based on an Immune Networks Model. *Journal of Wuhan University of Science and Technology(Natural Science Edition)*，29 (3), 313-315.

Dan Wu, Ken Chen. (2009). Design and Analysis of Precision Active Disturbance Rejection Control for Noncircular Turning Process. *IEEE Transactions on Industrial Electronics*, 50 (7), 2746-2753.

Han,J-Q. (2009). From PID to Active Disturbance RejectionControl. *IEEE Transactions on Industrial Electronics*, 56 (3), 900-906.

J. Han. (1999). Nonlinear design methods for control systems. *14th IFAC World Congress*, Proc.

Jingqing Han. (2008). *Active Disturbance Rejection Control Technique-the technique for estimating and compensating the uncertainties*. National Defense Industry Press，Beijing.

LI Hong-bin，Chen Lu. (2008). Fuzzy Immune PSD Control of Non-linear Systems. *Control Engineering of China*，15 (2), 168-170.

Liu Xing-qiao，Hu Jian-qun，Zhou li. (2010). Active Disturbance Rejection Control of Three-motor Synchronous Control System. *Proceedings of the CSEE*，30 (12), 81-85.

Liu Xingqiao，Tang Lin，Zhou li. (2012). Second-Order Active Disturbance Rejection Controller Applied in Three-Motor Synchronous System. *Transactions Of China Electrotechnical Society*，27 (2), 179-184.

Liu Xing-qiao，Tang Lin, Zhu Li-ting. (2013). Three-motor synchronous control system based on fuzzy active disturbances rejection control. *Electric Machines And Control*，17(4), 104-110.

Marco Pizzocaro, Davide Calonico, Claudio Calosso, et al. (2013). Active Disturbance Rejection Control of Temperature for Ultrastable Optical Cavities. *IEEE Transactions On Ultrasonics, Ferroelectrics, And Frequency Control*, 60 (2), 273-280.

Shihua Li, Cunjian Xia, Xuan Zhou. (2012). Disturbance rejection control method for permanent magnet synchronous motor speed-regulation system. *Mechatronics*, 22, 706-714.

Wang Li-jun, Tong Chao-nan, Li Qing, et al. (2012). A practical decoupling control solution for hot strip width and gauge regulation based on active disturbance rejection. *Control Theory & Applications*, 29 (11), 1471-1478.

Xia Changliang，Liu Dan，Wang Yingfa，et al. (2007). Control of Brushless DC Motors Using Fuzzy Set Based Immune Feedback PID Controller. *Transactions Of China Electrotechnical Society*，22 (9), 68-73.

Xingqiao Liu, Lin Tang, Li Zhou. (2011). Fuzzy Active Disturbance Rejection Control of Three-Motor Synchronous system. *Journal of Control Engineering and Applied Informatics*, 13 (4), 51-57.

Z. Gao, S. Hu, and F. Jiang. (2001). A novel motion control design approach based on active disturbance rejection. *40th IEEE Conf. Decision and Control*, vol.5, 4877-4882.

Z. Gao. (2003). Scaling and bandwidth-parameterization based on controller tuning. *American Control Conf.*, vol.6, 4989-4996.

Z. Gao. (2006). Active disturbance rejection control: A paradigm shift in feedback control system design. *American Control Conf.*, 2399-2405.